Zuschriften

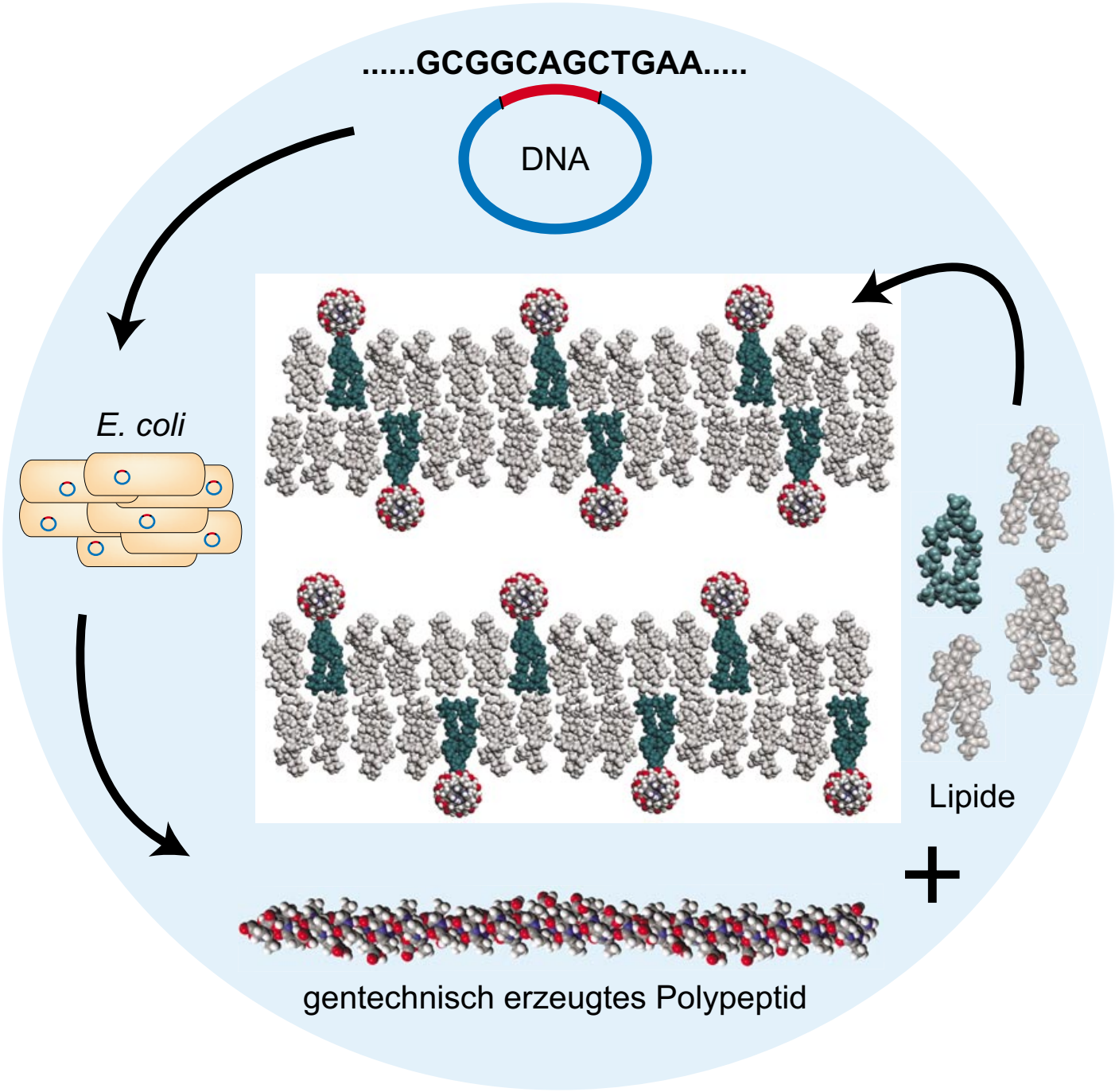

Gentechnisch erzeugte Polypeptide können sich mit entgegengesetzt geladenen Lipiden zu Materialien zusammenlagern, deren nanoskalige Ordnung auf mehreren Längenskalen eingestellt werden kann. Näheres hierzu finden Sie in der Zuschrift von I. Koltover et al. auf den folgenden Seiten.

DOI: 10.1002/ange.200460164

Nanostructures

Genetic Engineering of the Nanoscale Structure in Polyelectrolyte–Lipid Self-Assembled Systems**

Ilya Koltover, Sanjukta Sahu, and Nicolynn Davis*

The concept of molecular self-assembly has attracted interest in recent years as a route towards materials with structural order controlled on length scales from Ångstroms to micrometers. The assembly of macromolecules into ordered structures through noncovalent interactions has promise as an alternative to chemical synthesis; electrostatic, hydrophobic, and hydrogen-bonding interactions can be used to make equilibrium molecular structures with well-defined orientational and positional molecular order at the nanoscale without the need for complicated preparative procedures. An example of noncovalent self-assembly is the spontaneous formation of polyelectrolyte–lipid (PL) complexes in dilute solutions of polyelectrolytes and low-molecular-weight lipids,[1] with assembly driven by release of counterions from oppositely charged polymers and lipid head groups, as well as the hydrophobic association of the lipids. The resulting complexes usually have lamellar structures that consist of alternating lipid bilayers and adsorbed polyelecrolytes, although other mesophases can be obtained by tailoring the architecture of the surfactants.[2]

The utility of electrostatic self-assembly for making ordered nanomaterials is currently limited. Most known PL complexes have relatively disordered structures, with a small number of correlated polyelectrolyte/lipid layers (domain size) and no order among the polyelectrolyte chains sandwiched between membranes. Cationic lipid–DNA (CL–DNA) complexes are a notable exception, often having well-defined spacing among the DNA chains intercalated between the charged lipid membranes.[3] Thus, it is important to elucidate the requirements of polyelectrolyte architecture that are necessary to obtain a high degree of order in the PL complex. Herein, we report the formation of highly ordered PL complexes comprising cationic lipids and anionic polypeptides specifically designed and expressed in the bacterial host *Escherichia coli*. We demonstrate that when peptides have stable α-helical conformations with charge density matched to that of the cationic lipid membranes they form ordered PL complexes consisting of membrane stacks with peptide layers adsorbed on both surfaces of the membrane bilayers (Figure 1a). Furthermore, the peptide helices in the adsorbed monolayers form two-dimensional stripes, with the stripe thickness equal to the length of the monodisperse α helices, and well-defined interhelical spacing that can be varied by changing the composition of lipid membranes (Figure 1c, d). We demonstrate that control of polyelectrolyte molecular architecture opens a route to noncovalent self-assemblies with order on multiple length scales (Figure 1): lipid–polyelectrolyte stacking and two-dimensional order of the adsorbed polyelectrolytes.

DNA molecules have two distinctive features that may promote formation of the uniquely ordered CL–DNA structures. First, DNA has a well-defined double-helical fold that gives it rodlike shape and rigidity. Second, the area per anionic phosphate group of DNA is $\sigma^- = 68$ Å^2, with two helical lines of phosphate groups running along opposite sides of the DNA double helix.[4] This value is closely matched to the head-group size $\sigma^+ = 65$ Å^2 of the cationic lipid dioleoyl trimethylammonium propane (DOTAP), a fact contributing to the stability of a CL–DNA structure with layers of DNA binding together lipid bilayers in a stack. We hypothesized that a polypeptide with rigid shape and anionic charge density of $\sigma^- = 65$ Å^2 could also form ordered complexes with DOTAP-containing membranes. An α helix is the simplest rodlike peptide fold, and polypeptides with repetitive alanine-rich amino acid sequences are known to adopt stable helical conformations in aqueous solutions.[5] Hence, we chose to make PL complexes by using peptides with the sequence $(A_3E)_n$ (A = alanine, E = glutamic acid, n = integer). Molecular modeling studies of these peptides in α-helical conformation shows that the anionic glutamic acid residues are spaced at 6.5-Å intervals and are arranged on a helical line along the molecule axis;[6] with an α-helix diameter of 10 Å, this gives σ^- = ca. 65 Å^2, which is close to the desired charge density.

Helical folds of short (20–30 residue) peptides are unstable; they denature at temperatures of approximately 10 °C.[7] Therefore, we have used the methods of genetic engineering to prepare peptides of high molecular weight. DNA sequences (genes) encoding two polypeptides $(A_3E)_n$ with $n = 36$ and 48 were assembled from shorter synthetic oligonucleotides and inserted into bacterial expression plasmids in *E. coli* cells. Overexpression of these genes afforded two monodisperse polypeptides with precisely the expected molecular weights of 12.45 and 16.52 kDa.[8] The PL complexes precipitated as macroscopic globular aggregates from mixed solutions of these anionic peptides with cationic lipid vesicles. The vesicles comprised the cationic lipid DOTAP and the neutral lipid dioleoyl phosphatidylcholine (DOPC), and variation of the DOPC fraction (ϕ_{PC}) in the mixture was used to adjust the overall density of cationic lipids in the membrane bilayers. Stoichiometrically charge-neutral complexes were obtained by keeping the weight ratio of cationic DOTAP to anionic peptide at $\rho = 2$, since the molecular weight of DOTAP is twice that of the anionic A_3E repeat unit.[9]

The peptide conformations in solution and in the PL complexes were examined by using circular dichroism (CD)

[*] Prof. Dr. I. Koltover, S. Sahu, N. Davis
Department of Materials Science and Engineering
Northwestern University
Evanston, IL 60208 (USA)
Fax: (+1) 847-491-7820
E-mail: ilya@northwestern.edu

[**] Financial support for this research was provided by the National Sciences Foundation (grant no.: DMR-0134874) and the Petroleum Research Fund (grant no.: 37669-G7). X-ray experiments were carried out at the DND-CAT beam line of the Advanced Photon Source (ANL) facility supported by the DOE contract no. W-31-102-Eng-38.

Supporting information for this article is available on the WWW under http://www.angewandte.org or from the author.

  DOI: 10.1002/ange.200460164

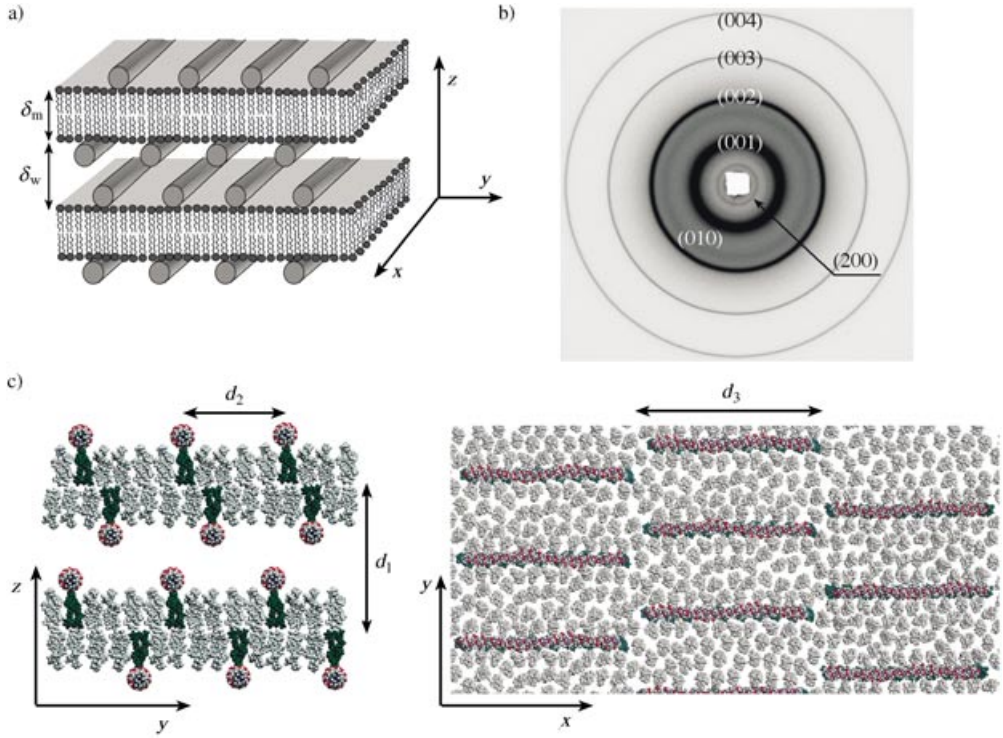

Figure 1. a) Schematic representation of the structure of the PL complex. b) SAXD pattern of the $(A_3E)_{48}$, $\rho = 2$, $\phi_{PC} = 0.75$ sample. c) and d) Molecular models of two projections of the structure of the PL complex; glutamic acid residues along the $(A_3E)_n$ α helices are shown in red, cationic DOTAP lipids are green, and neutral DOPC lipids are gray. For simplicity, $n = 18$ peptides were used to build the models.

spectroscopy (Figure 2). The CD spectra of pure peptides in solution show two minima at 208 and 223 nm and a maximum at 191 nm, a pattern characteristic of α-helical conformations. The peptides remained helical at room temperature (25 °C) and denatured into a random coil conformation above 40 °C. The CD spectra of dilute solutions of the PL complexes are nearly identical to those of pure peptides, a result indicating that they maintain a α-helical conformation inside the complexes.[10] Remarkably, the helical conformation of the peptides was stabilized in association with the cationic lipids, with strong helical CD signals for the PL complexes persisting at up to 70 °C.

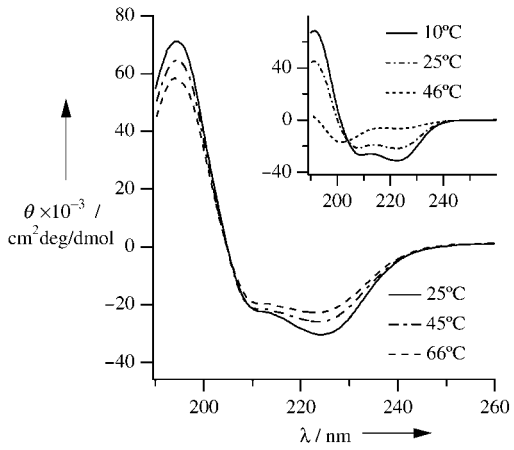

Figure 2. CD spectra of the $(A_3E)_{36}$, $\phi_{PC} = 0.7$, $\rho = 2$ complexes as a function of temperature in 10 mM sodium phosphate buffer (pH 6.5). The inset shows the CD spectra of pure $(A_3E)_{36}$ peptide solutions.

The nanoscale structure of the PL complexes was examined by using small-angle X-ray diffraction (SAXD) from concentrated aqueous suspensions of the complexes sealed in quartz capillaries.[10] Figure 1b shows a typical powder X-ray diffraction pattern of the PL complex with $n = 48$, $\rho = 2$, and $\phi_{PC} = 0.75$. Immediately apparent are the sharp periodically spaced (00*l*) rings, indicative of a highly periodic layered structure. Also visible is a diffuse (010) ring located between the first and second harmonics of the lamellar structure. Both the (00*l*) rings and the (010) ring were present in freshly prepared $\rho = 2$ complexes of either the $n = 36$ or $n = 48$ peptides with lipids for $\phi_{PC} > 0.5$, while only one or two rings at (00*l*) positions were visible in SAXD patterns of complexes with $\phi_{PC} < 0.5$.[11] Ordered complexes aged for several weeks yielded SAXD patterns with additional (*h*00) sharp reflections at very small angles, while the (00*l*) and (010) reflections remained unchanged.

To assign the three sets of X-ray diffraction peaks, we examined complexes with varying ϕ_{PC} and n (36 or 48) values. Figure 3a shows radially averaged plots of scattered X-ray intensity $I(q)$ for $(A_3E)_{36}$ samples with $\rho = 2$. The sharp (00*l*) peaks correspond to a PL complex with a highly periodic structure with stacked membrane and peptide/water layers along the *z*-axis (Figure 1). The stack periodicity $d_1 = 2\pi l/q_{00l}$ (where q = scattering vector) is equal to the sum of the membrane (δ_m) and peptide/water (δ_w) layer thicknesses. For a sample with $d_1 = 74.5$ Å and $\delta_m = 42$ Å ($\phi_{PC} = 0.8$),[3] the peptides occupy a space between the bilayers that is 32.5 Å

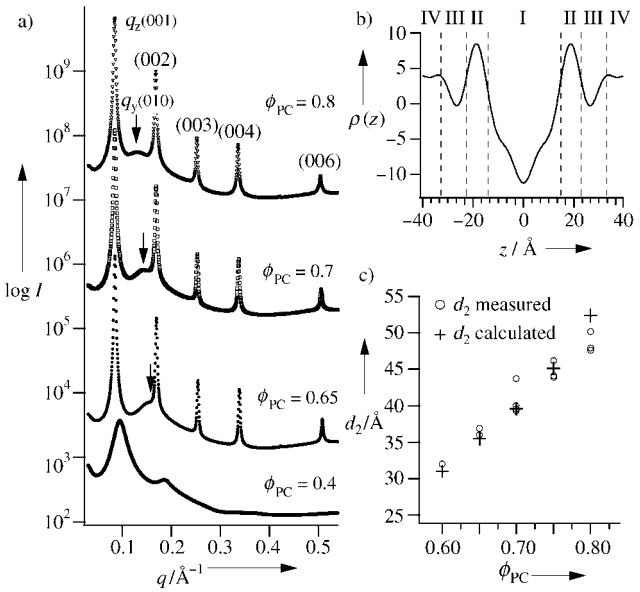

Figure 3. a) Radially averaged SAXD scans of $(A_3E)_{36}$, $\rho = 2$ samples; arrows indicate the shifting position of the interhelix-peptide correlation peak. Note the dramatic change in the data between the disordered ($\phi_{PC} < 0.5$) and ordered ($\phi_{PC} > 0.5$) samples. b) Electron density profile reconstructed from the SAXD scan for $\phi_{PC} = 0.8$. c) Variation of the interhelix-peptide spacing d_2 with the membrane composition ϕ_{PC} for all examined $(A_3E)_{36}$ and $(A_3E)_{48}$ samples; crosses indicate the d_2 values calculated with no adjustable parameters by using the space-filling model of PL complex shown in Figure 1.

thick. This is large enough to accommodate two layers of peptides with a diameter of 10 Å, with a water layer between them. Inversion of the X-ray data reveals a projected electron-density profile $\rho(z)$ with four distinct electron-density regions I–IV (Figure 3b).[12] Region I has a $\rho(z)$ profile characteristic of a hydrophobic lipid-bilayer interior, with an adjacent higher density layer (II) that corresponds to the lipid head groups. Peptides are adsorbed on both surfaces of the lipid bilayer, thereby giving rise to region III with a reduced $\rho(z)$ value because the carbon/nitrogen composition of the peptide results in electron density that is somewhat lower than that of the water layer (IV). The measured $\rho(z)$ pattern exactly corresponds to the repeating bilayer/peptide unit of the PL stacked structure shown in Figure 1.

The observed stack structure is different from the CL–DNA complexes, where DNA molecules bridge the neighboring membrane layers. However, DNA has two sets of anionic groups running along its double strand, while the helical (A_3E) peptides have a single row of charges that can efficiently neutralize only a single membrane surface. Furthermore, since at most half of the peptide charged groups face towards the membrane surface and interact directly with cationic lipid head groups, efficient charge neutralization can only occur for membranes with average charge density $\sigma^+ = 2 \times 65$ Å^2, which is two times lower than the expected geometric value. Thus, complexes with $\phi_{PC} < 0.5$ have disordered structures (bottom curve in Figure 3a) because of inefficient screening of the membrane charges by the adsorbed anionic peptides.

The average distance between the adsorbed peptide helices can be estimated from the ratio of peptide to membrane charge densities as $d_2 = (1\,e^-$ per 6.5 Å$)/(1\,e^+$ per 65 Å$^2 \times \phi_{TAP}) = 10/(1-\phi_{PC})$, which corresponds to $d_2 =$ ca. 50 Å for $\phi_{PC} = 0.8$. This value is close to the measured value of $d_2 = 2\pi/q_{010} = 48$ Å, a result suggesting that the broader (010) reflection arises from well-defined side-by-side ordering of the polypeptide chains. As expected, the (010) peak moves to smaller angles for samples with increasing ϕ_{PC} values (Figure 3a, c). A better estimate of $d_2(\phi_{PC})$ values can be obtained by matching the volumes occupied by membranes and peptides in the structure shown in Figure 1b (see the Supporting Information). Figure 3c shows the remarkable agreement between calculated d_2 values and the measured data. This further verifies the proposed structure of the PL complex and also shows that the well-defined ordering of adsorbed peptide helices can be experimentally controlled by adjusting the membrane composition.

The origin of the additional $(h00)$ reflections in aged samples of the PL complex was investigated by comparing the diffraction patterns in samples of peptides with different n values; these patterns were obtained by using a diffraction set-up capable of accessing smaller scattering angles. Figure 4 shows a set of radially averaged SAXD scans in the small-angle region for three $(A_3E)_{48}$ and two $(A_3E)_{36}$ samples with varying ϕ_{PC} values. It is clear that the positions of the $(h00)$ harmonics change dramatically for the samples with different peptide lengths. The expected lengths of α helices with 36 and 48 residues are 216 and 288 Å (1.5 Å $\times n$), respectively. Thus, the period d_3 of $(h00)$ reflections is essentially equal to the

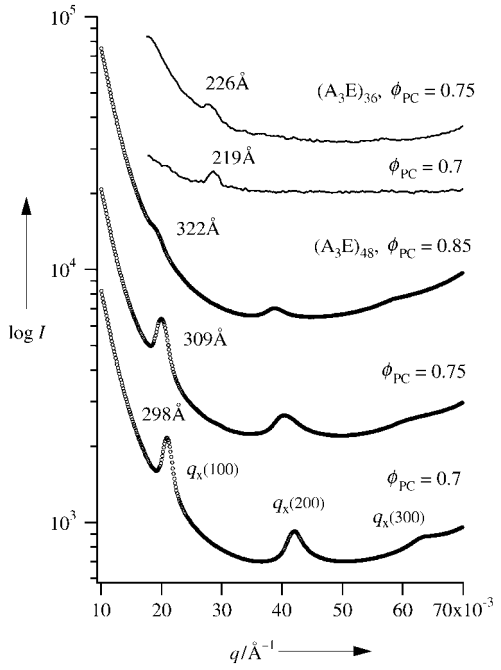

Figure 4. Small-angle diffraction region of aged samples of the PL complex. The bottom three scans are for $(A_3E)_{48}$, $\rho = 2$ samples; the top two scans are for $(A_3E)_{36}$, $\rho = 2$ samples. The noisier $(A_3E)_{36}$ data were recorded on a lower-resolution diffraction set-up. Numbers above the diffraction curves indicate the periodicity $d_3 = 2\pi/q_{100}$ of the corresponding data.

peptide length. This means that the helical peptides slowly separate into two-dimensional stripes on the surfaces of lipid membranes. The stripe period d_3 is proportional to the helix length, and there is well-defined spacing (d_2) between helices in each stripe (Figure 1c). The small increase in the d_3 distance with increasing ϕ_{PC} value indicates that the stripes move slightly apart as the membrane charge density decreases.

It is likely that the separation of monodisperse peptides and associated cationic lipids into stripes reduces the thickness perturbation and elastic energy of the lipid membranes compared to a random peptide distribution along the *x*-axis. The X-ray peaks with a striped pattern appear in aged samples because two-dimenional diffusion of lipids with adsorbed peptides is slow. SAXD measurements show no correlations between peptide arrays on different membrane surfaces or between peptide positions in neighboring stripes. Importantly, the observed two-dimensional ordering of peptide chains is possible only as a consequence of the perfect monodispersity and uniform conformation of the genetically engineered polypeptide chains.

In summary, we have shown that highly ordered noncovalent self-assemblies can be prepared from cationic lipids and genetically engineered polypeptides. Our results demonstrate that polyelectrolyte conformation and charge density are the key design parameters for engineering order in PL self-assembled systems. It is important to note that the structure of the PL complex is essentially encoded in the DNA sequences, which prescribe the α-helical fold, charge density, and length of the molecules by establishing the sequence and length of the biosynthetic peptides. This synthetic strategy mimics the way that nature guides self-assembly through the use of genetically encoded, well-defined macromolecules.

Received: March 31, 2004 [Z460164]
Published Online: July 28, 2004

Keywords: amphiphiles · lipids · nanostructures · polyelectrolytes · self-assembly

[1] a) M. Antonietti, J. Conrad, A. Thunemann, *Macromolecules* **1994**, *27*, 6007; b) M. Antonietti, J. Conrad, *Angew. Chem.* **1994**, *106*, 1927; *Angew. Chem. Int. Ed. Engl.* **1994**, *33*, 1869; c) E. A. Ponomarenko, A. J. Waddon, K. N. Bakeev, D. A. Tirrell, W. J. MacKnight, *Macromolecules* **1996**, *29*, 4340; d) J. O. Radler, I. Koltover, T. Salditt, C. R. Safinya, *Science* **1997**, *275*, 810; e) G. Subramanian, R. P. Hjelm, T. J. Deming, G. S. Smith, Y. Li, C. R. Safinya, *J. Am. Chem. Soc.* **2000**, *122*, 26; f) G. C. L. Wong, J. X. Tang, A. Lin, Y. L. Li, P. A. Janmey, C. R. Safinya, *Science* **2000**, *288*, 2035.

[2] a) I. Koltover, T. Salditt, J. O. Radler, C. R. Safinya, *Science* **1998**, *281*, 78; b) S. Zhou, F. Yeh, C. Burger, B. Chu, *J. Phys. Chem. B* **1999**, *103*, 2107; c) R. Krishnaswamy, P. Mitra, V. A. Raghunathan, A. K. Sood, *Europhys. Lett.* **2003**, *62*, 357.

[3] I. Koltover, T. Salditt, C. R. Safinya, *Biophys. J.* **1999**, *77*, 915.

[4] D. Voet, J. G. Voet, *Biochemistry*, Wiley, New York, **1995**, p. 852.

[5] S. Marqusee, V. H. Robbins, R. L. Baldwin, *Proc. Natl. Acad. Sci. USA* **1989**, *86*, 5286.

[6] Molecular models of peptides and lipid/peptide assemblies were built by using the Materials Studio (Accelrys) package. Peptides were constructed by using conventional 18/5 α-helix dihedral angles. The structures were not minimized and were used as a guide for molecule design and structure visualization.

[7] J. M. Sholtz, H. Qiang, E. J. York, J. A. Stewart, R. L. Baldwin, *Biopolymers* **1991**, *31*, 1463.

[8] Details of peptide gene cloning, peptide expression and purification, and sample preparation can be found in the Supporting Information.

[9] All experiments performed with complexes prepared in water and 10 mM sodium acetate or sodium phosphate buffers (pH 6.5) yielded identical results. Furthermore, CD and SAXD data were identical for $(A_3E)_{36}$ and $(A_3E)_{48}$ samples, except the (*h*00) reflections in the very-small-angle diffraction region.

[10] Samples for CD experiments were prepared from dilute solutions of peptides ($0.25\,mg\,mL^{-1}$) and liposomes ($0.5\,mg\,mL^{-1}$). SAXD samples were prepared directly in 2 mm diameter quartz X-ray capillaries from peptide ($50\,mg\,mL^{-1}$) and liposome ($100\,mg\,mL^{-1}$) stock solutions.

[11] The difference between the $\phi_{PC} < 0.5$ (disordered) and $\phi_{PC} > 0.5$ (ordered) samples was also evident from their visual appearance: ordered samples consisted of compact, strongly birefringent globules, while the disordered ones had faint, weakly birefringent aggregates. See the Supporting Information for an example.

[12] a) H. Richardsen, U. Vierl, G. Cevc, W. Fenzl, *Europhys. Lett.* **1996**, *34*, 543; b) N. P. Franks, W. R. Lieb, *J. Mol. Biol.* **1979**, *133*, 469; intensities of the first six (00*l*) peaks were used for the reconstruction; the phases (−1, −1, −1, 1, −1, −1) were chosen based on the known reconstructions of pure lipid structures, with rejection of unphysical electron density profiles.

